

Article Type: Original Article

Manuscript Category: Signaling & Cell biology (SCB)

T-type calcium channels drive migration/invasion in BRAFV600E melanoma cells through Snail1

Maiques O^{1†}, Barceló C^{1†}, Panosa A¹, Pijuan J¹, Orgaz JL⁴, Rodriguez-Hernandez I⁴, Matas-Nadal C², Tell G⁷, Vilella R⁵, Fabra A⁶, Puig S⁷, Sanz-Moreno V⁴, Matias-Guiu X³, Canti C¹, Herreros J¹, Marti RM^{2§}, Macià A^{1§*}

¹University of Lleida, IRBLleida, Lleida, Spain. Departments of ²Dermatology, ³Pathology and Molecular Genetics, Hospital Universitari Arnau de Vilanova, University of Lleida, IRBLleida, Lleida, Spain. Centre of Biomedical Research on Cancer (CIBERONC), Instituto de Salud Carlos III (ISCIII), Spain. ⁴Tumour Plasticity Laboratory, Randall Division of Cell and Molecular Biophysics, New Hunt's House, Guy's Campus, King's College London, London SE11UL, UK. ⁵Department of Immunology, Hospital Clínic, Barcelona, Spain. ⁶Molecular Oncology, Bellvitge Biomedical Research Institute (IDIBELL), L'Hospitalet de Llobregat, Barcelona, Spain.

⁷Melanoma Unit, Department of Dermatology, Hospital Clínic de Barcelona, Institut d'Investigacions Biomèdiques August Pi i Sunyer (IDIBAPS), University of Barcelona, Barcelona, Spain. Centre of Biomedical Research on Rare Diseases (CIBERER), Instituto de Salud Carlos III (ISCIII), Spain.

*corresponding author. E-mail: amacia@irbllleida.cat

†OM and CB are first authors and [§]RMM and AM are senior authors

This article has been accepted for publication and undergone full peer review but has not been through the copyediting, typesetting, pagination and proofreading process, which may lead to differences between this version and the Version of Record. Please cite this article as doi: 10.1111/pcmr.12690

This article is protected by copyright. All rights reserved.

ABSTRACT

Melanoma is a malignant tumor derived from melanocytes. Once disseminated, it is usually highly resistant to chemotherapy and is associated with poor prognosis. We have recently reported that T-type calcium channels (TTCCs) are overexpressed in melanoma cells and play an important role in melanoma progression. Importantly, TTCC pharmacological blockers reduce proliferation and deregulate autophagy leading to apoptosis. Here, we analyze the role of autophagy during migration/invasion of melanoma cells.

TTCC Cav3.1 and LC3-II protein are highly expressed in BRAFV600E compared to NRAS mutant melanomas, both in cell lines and biopsies. Chloroquine, pharmacological blockade or gene silencing of TTCCs inhibits the autophagic flux and impairs the migration and invasion capabilities, specifically in BRAFV600E melanoma cells.

Snail1 plays an important role in motility and invasion of melanoma cells. We show that Snail1 is strongly expressed in BRAFV600E melanoma cells and patient biopsies, and its expression decreases when autophagy is blocked. These results demonstrate a role of Snail1 during BRAFV600E melanoma progression and strongly suggest that targeting macroautophagy and, particularly TTCCs, might be a good therapeutic strategy to inhibit metastasis of the most common melanoma type (BRAFV600E).

SIGNIFICANCE

T-type calcium channels (TTCCs) are overexpressed during melanoma progression, but the role they play is still unclear. The present study reports an impairment of migration and invasion abilities of the most common genetic melanoma subgroup (BRAF/V600E) when subjected to pharmacological TTCC blockade. It has been long described that BRAF/V600E melanomas have upregulated autophagic flux, and similar results have been observed when autophagy is blocked. These findings show that autophagy and TTCC regulation intersect at some point which seems to be controlled by Snail1. Therefore, the present work is at the frontier between basic and translational science and open new therapeutic strategies.

INTRODUCTION

Cutaneous melanoma is a malignant neoplasm derived from skin melanocytes. Melanoma cells have a high ability of local invasion and metastasis, even when arise from very small volume tumors (Gray-Schopfer, Wellbrock, & Marais, 2007). Once disseminated, melanoma is highly resistant to conventional anticancer treatments and its prognosis is poor (Pollack et al., 2011). As melanoma can present in young and medium age adults (Lee et al., 2016; Ríos et al., 2013), it causes disproportionate mortality in such population being responsible of one of the highest rate of loss of potential life for adult-onset cancers (Ekwueme et al., 2011). Although available therapies for metastatic melanoma have evolved substantially in the last years, especially with the introduction of targeted- and immunotherapies (M. Hao et al., 2015), melanoma is still a serious health care problem and melanoma cell behavior is an important subject of research.

Several genetic mutations have been associated to melanoma development and progression. Overall, around 40-50% of melanomas carry mutations in the *BRAF* gene. Of these, 90% bear the *BRAFV600E* mutation (Banzi et al., 2016; Dhomen et al., 2009). About 20% of melanomas harbor mutations in the *NRAS* gene, mostly affecting codon Q61 (Jakob et al., 2012). Moreover, many other genetic alterations have been described that confer gain/loss function of genes that trigger abnormal signaling pathways like KIT, GNAQ/GNA11, CDKN2A, PTEN, NF1, BAP1, among others (Griewank et al., 2014). Some studies advocate that patients with primary *BRAFV600E* or *NRAS* melanoma have worse survival rate compared to wild-type (WT) *BRAF* melanoma patients (Davies et al., 2002; Long et al., 2011). However it seems that, once disseminated, *BRAF* and *NRAS* mutation status does not influence survival in metastatic melanoma (Carlino et al., 2014).

The expression of T-type calcium channels (TTCCs) is increased in a number of tumors, where they promote cell proliferation (Dziegielewska, Gray, & Dziegielewski, 2014; Macià, Herreros, Martí, & Cantí, 2015). Human melanoma cells overexpress Cav3.1 and Cav3.2 isoforms of TTCCs, compared with untransformed melanocytes (A Das et al., 2012). Importantly, TTCC pharmacological blockers not only reduce the proliferation of melanoma cells, but also trigger apoptotic cell death, partially through the activation of caspases (Arindam Das et al., 2013). We found that such apoptotic process is preceded by ER stress and blockade of the autophagic flux (Arindam Das et al., 2013). Therefore, TTCCs may be valuable therapeutic targets against melanoma progression (A Das et al., 2012; Arindam Das et al., 2013; Macià et al., 2015; Maiques et al., 2016).

Macroautophagy (hereafter autophagy) is a housekeeping cell process that plays a significant role in tumor progression (Kroemer, Mariño, & Levine, 2010; Mizushima & Komatsu, 2011) and

Accepted Article

resistance to therapy (Amaravadi, 2011; Corazzari et al., 2015; Ma et al., 2011). Autophagy is constitutively induced in melanoma cells, and may be further induced during chemotherapy (Corazzari et al., 2015; Arindam Das et al., 2013; Ma et al., 2011). In addition, autophagy blockade results in decreased tumor cell migration and invasion (Lu et al., 2016; Mowers, Sharifi, & Macleod, 2016; Sharifi et al., 2016). Hence, autophagy modulation is an emerging therapeutic strategy also in melanoma.

Melanoma cell invasion and subsequent metastasis are hallmarks of melanoma dissemination (Chin, Garraway, & Fisher, 2006). Snail1 is a major transcription factor that induces epithelial-mesenchymal transition (EMT) and has been shown to be crucial during tumor progression and invasion (Cano et al., 2000; Thiery, 2002). In melanoma cells, Snail1 is up-regulated (Poser et al., 2001) and promotes cell motility and invasiveness (L. Hao, Ha, Kuzel, Garcia, & Persad, 2012; Olmeda, Jordá, Peinado, Fabra, & Cano, 2007). Consequently, downregulation of Snail1 in melanoma cells reduces tumor growth, metastasis and immunosuppression (Kudo-Saito, Shirako, Takeuchi, & Kawakami, 2009; Pearlman, Montes de Oca, Pal, & Afaq, 2017).

RESULTS

Expression of TTCCs in melanoma cells with different genetic profile.

We first studied the expression of TTCCs by RT-PCR in a wide range of melanoma cell lines bearing different molecular features (Table S1). Different levels and patterns were observed in all melanoma cell lines regarding transcripts for Cav3.1 (Figure 1a), Cav3.2 (Figure 1b) and Cav3.3 (Figure 1c) isoforms. However, Cav3.1 levels were frequently higher than in untransformed melanocytes (HEMn-LP). The expression of Cav3.1 and Cav3.3 mRNA was increased in BRAFV600E melanoma cell lines compared to NRASQ61H/K/L/R (Figure 1d- f), whereas no significant differences were observed regarding to Cav3.2 mRNA levels (Figure 1e).

TTCC blockers block basal autophagy in all melanoma cell lines

Autophagy in melanoma cells is constitutively active (Arindam Das et al., 2013; Maes & Agostinis, 2014). To study autophagy, we measured LC3I/II, an autophagic marker (Sahani, Itakura, & Mizushima, 2014), by Western blot (WB) in melanoma cell lines. We observed an increase of LC3II levels in most of the BRAFV600E melanoma (Figure 1g). When cells were treated with TTCC blockers (Mibefradil (Mib) and Pimozide (Pim)) increased levels of LC3II and p62 were detected in BRAFV600E (Figure 1h, S1a) and NRAS (Figure 1i, S1b) melanoma cell

lines. This data is suggestive of autophagy blockade at a step following autophagosome biogenesis. Treatment of the melanoma cell lines with Chloroquine (CQ), that prevents the fusion of autophagosomes (AP) with lysosomes (Boya et al., 2005), led to similar increases of LC3II and p62 proteins in all cell lines (Figure 1j-1k, S1c-d). To further confirm these changes on autophagy observed by western blot, LC3B immunofluorescence (IF) was used as a marker for AP (Mizushima, Yoshimori, & Levine, 2010). A significant increase of AP *puncta* was observed both in M3 (BRA^{FV600E}) and in Skmel-147 (NRAS^{Q61R}) cell lines when they were subjected to Mib or CQ treatment (Figure 1l). Moreover, addition of Chloroquine to Mibefradil-treated cultures did not further increase the levels of p62 and LC3II (Figure S1e). Taken together, these results indicate that TTCC blockers block autophagy, regardless of the specific mutation present in melanoma cell lines.

Autophagy blockade inhibits collective migration of BRA^{FV600E} melanoma cell lines

Cell migration is a key process during melanoma metastasis. We assessed the effect of TTCC blockers on melanoma migration using a wound healing assay that measures collective migration. Both TTCC blockers decreased the percentage of BRA^{FV600E} melanoma cells migrating into the wound (Figure 2). Consistently, treatment of BRA^{FV600E} cell lines with CQ also reduced the migration rate (Figure 2a-b, S2a-c). Interestingly, migration was unaffected in NRAS mutant melanoma cells treated with TTCC blockers or CQ (Figure 2c-d, S2d-f) even when autophagy was blocked.

Using time-lapse microscopy, we found slower migration of BRA^{FV600E} cells (M3 and M249) treated with Mibefradil or CQ when compared to control, even after 8h treatment (Figure S3a-b). Furthermore, the healing speed of BRA^{FV600E} cells decreased after treatment with either Mibefradil or CQ (Figure 2a-b, S3a-b and movies S1-3 (M3)).

In contrast, Mibefradil or CQ treatments did not affect neither the percentage of wound healing nor the healing speed of the NRAS mutant cells (Figure 2c-d, S3c-d and movies S4-6 (Skmel147)).

To further study how autophagy inhibition affects melanoma cell migration, we knocked down Atg5, an autophagy-related protein required for autophagosome formation (Pyo et al., 2005), by lentivirus-driven shRNA. Silencing of Atg5 induced a decrease of LC3II in both BRA^{FV600E} and NRAS mutant cell lines (Figure 2e). It also decreased the migration of BRA^{FV600E} (M3) melanoma cells (Figure 2f), but not of the NRAS mutant cells (WM-1366) (Figure 2g).

Overall, these results show that the BRAFV600E cell lines are less motile after treatment with Mibefradil, Pimozide, CQ, or silencing Atg5 expression, suggesting that TTCC blockers inhibit the migration of BRAFV600E cells by blocking the autophagic process.

Mibefradil and CQ inhibit single cell migration in BRAFV600E melanoma cells.

To analyze the effect of TTCC blockers on cell migration independent of cell-cell interactions, we studied single cell random migration by time-lapse. For these experiments, melanoma cells were plated at lower density compared to previous approaches and Mibefradil and CQ concentrations were halved (12.5 μ M and 5 μ M, respectively) in order to maximize cell survival and also halted basal autophagy (Figure S4). Analysis of individually tracked cells revealed that the accumulated distance and the migration speed of BRAFV600E cells were significantly reduced when treated with Mibefradil or CQ (Figure 3a-b, movies S7-9 (M3)). In line with our findings, neither the distance nor the velocity was significantly affected by either treatment in NRAS mutant cells (Figure 3c-d, movies S10-12 (Skmel147))

This results show that Mibefradil and CQ decrease single cell migration in BRAFV600E melanoma cells by blocking the autophagic flux.

Autophagy blockade inhibits invasion of BRAFV600E melanoma cell lines.

We next investigated the effect of TTCC blockers on the invasive capacity of melanoma cells. Treatment with Mibefradil or CQ for 24h inhibited the invasive capacity of BRAFV600E melanoma cells (Figure 4a-b). Similar results were observed upon 24h treatment with Pimozide (Figure S5a-b). On the contrary, neither TTCC blockers nor CQ affected the invasion ability of the NRAS mutant cell lines (Figure 4a-b). Silencing Atg5 expression (Figure 2e) also reduced the invasive capacity of BRAFV600E (M3) melanoma cells. Again, differences were not significant in NRAS (WM-1366) mutant cells (Figure 4c-d). These results indicate that autophagy inhibition or blockade might be used to control the invasive potential of BRAFV600E melanoma cells.

Gene silencing of TTCCs reduces the invasion ability of BRAFV600E melanoma cell lines

Previously we showed that TTCC silencing leads to autophagy impairment that mimics the effect of TTCC blockers (Arindam Das et al., 2013). To investigate the possible involvement of TTCCs in the invasion capacity of BRAFV600E melanoma cells, we knocked down TTCCs in M3 cells using lentiviral constructs carrying shRNA specific to Cav3.1 and Cav3.2 (Figure S5c-e). When measured in Transwell assays, both TTCC silencing inhibited the invasive capability of

M3 cells (Figure 4e-f). An increase of p62 and LC3II protein levels was observed when either Cav3.1 or Cav3.2 isoforms were silenced (Figure S5f), thus mimicking the effects of Mibefradil, Pimozide or CQ. These results indicate that TTCCs leads to induce invasion in BRAFV600E melanoma cell lines.

Analysis of expression of TTCCs in biopsies from melanoma patients

To extend our observations to the clinical settings, we used a cohort of 33 primary and 28 metastatic melanomas biopsies. Such cohort was divided in two main groups according to their BRAF genetic status (mutant BRAFV600E/K vs BRAFWT) analyzed by PCR sequencing (Table S2). The expression levels (histoscore) of TTCCs (Cav3.1 and Cav3.2) and LC3 were assessed by IHC. All melanoma samples bearing BRAFV600E/K gene mutations showed a higher immunoexpression of Cav3.1 compared to the WT BRAFWT cohort (Figure 5a-b), thus confirming our previous results (Maiques et al., 2016). In contrast, Cav3.2 immunoexpression did not show significant differences between the two groups (Figure 5c-d).

We additionally checked whether the mutation status of melanoma cells had an impact on macroautophagy, by quantifying the expression of LC3. The immunoexpression of LC3 was elevated in the BRAFV600E/K biopsies compared to the BRAFWT group (Figure 5e-f), suggesting an enhanced basal autophagy of BRAFV600E/K biopsies.

Snail1 expression is higher in BRAFV600E melanomas and decreases upon autophagy blockade

Snail1 plays several roles in cell migration and EMT process (Cano et al., 2000). To understand if autophagy was regulating cell migration and invasion controlling Snail1 we quantified the expression of Snail1 in our melanoma cell lines by WB and RT-PCR, and found that both protein (Figure 6a) and mRNA (Figure 6b) levels were augmented in BRAFV600E, compared to NRAS mutant cells.

Snail1 was reduced in BRAFV600E cell lines that were treated with TTCC blockers (Figure 6c), or subjected to gene silencing of TTCCs (Figure 6f). In addition, treatment of BRAFV600E cells with CQ (Figure 6d) or gene silencing of ATG5 (Figure 6e) consistently decreased the levels of Snail1, showing that the expression of Snail1 was related to the status of the autophagic flux. It has been shown that Snail1 plays an important role in melanoma progression (L. Hao et al., 2012; Olmeda et al., 2007). Indeed, Snail1 knockdown impaired cell migration and invasion (Figure 6g-h) of BRAFV600E cells, mimicking the effect of TTCC blockers and CQ. To further study whether Snail1 can modulate autophagy in melanoma cells, we stably overexpressed Snail1

(PLX-Snail1) in an NRAS mutant cell line, SKMEL147. Snail1 overexpression induced an increase in p62 and LC3I/II levels compared to PLX-empty vector cells (Figure 6i). Moreover, immunofluorescence of LC3B showed a slightly increase of AP *puncta* when Snail1 was overexpressed and such increase was higher after a short treatment of CQ, suggesting a possible increase of basal autophagy. In addition, Mibefradil treatment increased LC3B positive *puncta* in cells, independently on Snail1 expression (Figure 6j).

To investigate whether Snail1 takes part in migration/invasion process during modulation of autophagic flux, we treated Snail1-overexpressing cells with Mib or CQ. There was an impairment of migration (Figure 6k) and invasion (Figure 6m) in Snail1-overexpressing cells when autophagy was blocked. Furthermore, Mibefradil decreased single cell migration in Snail1-overexpressing cells (Figure 6l). These results suggest that Snail1 could be essential to impair migration/invasion when autophagy is blocked, particularly by targeting TTCCs. To complement these approaches, we used the publicly available database TCGA and found that Snail1 expression was increased in melanoma biopsies of patients harboring BRAFV600E mutation, compared to that BRAFWT (Figure 6n). Cell migration and invasion are key steps during metastatic dissemination; therefore, we performed Snail1 IHC analysis in metastatic vs primary melanoma biopsies. Snail1 nuclear staining (active form) was significantly higher in metastatic compared to primary lesions only in patients harboring BRAFV600E/K mutations (Figure 6o). Moreover, we observed a higher Snail1 score in BRAFV600E/K metastasis, compared to BRAFWT metastatic tumors. These results indicate an important role of Snail1 during metastatic spread of BRAFV600E melanomas.

DISCUSSION

We have previously shown that the immunoexpression of TTCCs increases gradually from melanocytes to primary and metastatic melanoma biopsies and relates to poor prognosis (Maiques et al., 2016). Here we describe (in both cultured cell lines and FFPE melanoma biopsies) that the Cav3.1 isoform is upregulated in BRAFV600E melanomas, which is accompanied by increased levels of LC3-II proteins, compared to NRAS mutant. BRAFV600E melanoma cells display an enhanced autophagy (Armstrong et al., 2011; Corazzari et al., 2015; Giglio, Fimia, Lovat, Piacentini, & Corazzari, 2015; Maddodi et al., 2010). Thus, autophagy inhibition could be a therapeutic tool to enhance the antitumor activity of BRAF inhibitors. Furthermore, this strategy may also prevent tumor resistance, as autophagy preceded by ER stress is a likely mechanism of resistance to BRAF inhibitors in melanoma (Ma et al., 2014). In

Accepted Article

support of this, combination of Atg5 knockdown and MEK inhibition increases cell death in vemurafenib-resistant melanoma cell lines (Martin et al., 2015).

Importantly, autophagy also plays a role in melanoma metastasis. For instance, Xie et al. showed that autophagy inhibition by deletion of Atg7 or treatment with CQ suppresses melanoma tumor growth and increases survival of mice driving oncogenic BRAFV600E expression and Pten-deficiency in melanocytes (Xie, Koh, Price, White, & Mehnert, 2015). Furthermore, CQ reduces tumor growth and impairs melanoma cell invasion and metastasis (Maes et al., 2014). In addition, Sharifi and co-workers revealed that autophagy inhibition reduces cell migration and invasion (in breast cancer and melanoma) and attenuates the induction of metastasis by disrupting the focal adhesion turnover (Sharifi et al., 2016). We studied the role of autophagy in the migration/invasion of BRAFV600E and NRAS melanomas. Our results demonstrate that TTCC blockers, Mibefradil and Pimozide, impair migration and invasion of BRAFV600E cells, an effect exerted also by CQ or Atg5 knockdown. In contrast, cell motility *in vitro* is largely unaffected by autophagy inhibition in NRAS melanoma cell lines.

We evaluated Snail1 expression, a master transcription factor that induces EMT and invasion in melanoma cells (L. Hao et al., 2012; Olmeda et al., 2007). Our results indicate that Snail1 expression is higher in BRAFV600E melanoma cells compared to BRAFWT cells. Interestingly, Snail1 levels decrease when autophagy is blocked by chloroquine or by TTCC blockers, thus inhibiting migration and invasion. Furthermore, when we overexpressed Snail1 in NRAS mutant melanoma cell line, we show an impairment of migration/invasion abilities when autophagy is blocked. Therefore, autophagy appears to regulate cell motility through different mechanisms depending on the cell type and context (Kenific, Thorburn, & Debnath, 2010).

BRAF and NRAS mutations are mutually exclusive in melanoma (Davies et al., 2002). Common to them is the direct or concomitant hyperactivation of signaling pathways like MEK-ERK and PI3K (Griewank et al., 2014; Vu & Aplin, 2016). However, our studies indicate that BRAFV600E and NRASQ61 activate distinct cellular mechanisms related to melanoma progression. It has been shown that activation of ERK, the main target of BRAFV600E, is an upstream signaling mechanism responsible for high constitutive Snail1 expression in melanoma cells (Massoumi et al., 2009). In addition, Snail1 knockdown disrupts tumor growth and impairs melanoma progression and migration, similar to results reported here (L. Hao et al., 2012; Massoumi et al., 2009). In BRAFV600E melanomas, the phosphorylation of Cortactin and the exocyst subunit Exo70 upon ERK activation, which regulates the secretion of matrix metalloprotease-2, appears as a relevant mechanism for cell migration (Lu et al., 2016; Sandri et al., 2016).

Our findings reveal an unknown link between autophagy and Snail1 expression that regulates the migration and invasion of BRAFV600E melanoma cells. It has been described that p62 modulates the stability of Snail1, a mediator of TGF β /Smad signaling, through its UBA domain (Bertrand et al., 2015). New evidences indicate that autophagy is not only involved in the intracellular degradation of damaged proteins, but also plays an important role in protein secretion (Kraya et al., 2015; Narita et al., 2011). In addition, autophagy-related secretion affects the tumor microenvironment and reflects the autophagy dynamics of tumor cells (Kraya et al., 2015). A recent paper further revealed that the TGF β /Snail signaling pathway induces EMT-like process in a paracrine manner in melanoma (Lv et al., 2017). Moreover, knockout mice of GABARAP, an Atg8/LC3 family member implicated in the induction of autophagy, showed reduced amounts of TGF β in serum and inhibition of tumor initiation and progression, through the enhancement of both anti-tumor immunity and cell death signaling (Salah et al., 2016). Therefore, all these data may suggest that the secretion of TGF β through autophagy could lead to increased expression of Snail1, during the induction of migration/invasion of BRAFV600E melanoma cells. Nevertheless, the mechanism by which Snail1 levels decrease upon autophagy blockade in BRAFV600E melanoma cells requires further investigation. A possibility would be that Snail1 proteasomal degradation (Muqbil, Wu, Aboukameel, Mohammad, & Azmi, 2014) is deregulated after autophagy blockade.

In conclusion, our findings indicate that BRAV600E melanoma cells display higher levels of the Cav3.1 TTCC and an increased basal autophagy, compared to other types of melanoma cells. In addition, the migration and invasion capabilities of BRAFV600E cells are sensitive to the genetic ablation or pharmacological inhibition of autophagy and depend on Snail1 levels. Thus, chemotherapeutic strategies targeting TTCCs and/or autophagy appear especially suitable to tackle metastasis in the most common type of melanoma.

MATERIALS AND METHODS

Cell lines

Twelve human malignant melanoma cell lines were used and sequenced (BRAF or NRAS mutation) (Table S1). For cell culture conditions see Supplemental Experimental Procedures.

Real-time RT-PCR

Total RNA was extracted with a SurePrep Total RNA Isolation kit (Applied Biosystems). Total RNA 2 μ g was used to generate cDNA with Taqman technology from Applied Biosystems. Relative expression was calculated using the comparative $\Delta\Delta$ CT method. Levels of both calcium channels were expressed as fold change relative to mRNA from melanocytes (HEMn-LP). Probes used are detailed in Supplemental Experimental Procedures.

Western blot

Melanoma cells were lysed in 2% sodium dodecyl sulfate (SDS), 125 mM Tris-HCl, pH 6.8. Western blot was conducted as described (Arindam Das et al., 2013). The antibodies used are detailed in Supplemental Experimental Procedures.

Immunofluorescence

Melanoma cells were fixed with 100% methanol (10min 4°C), and blocked with 0.2% Triton X-100 (1h RT). Cells were incubated with anti-MAP1LC3B (1:200, rabbit polyclonal, Cell Signaling Technology, 4°C o/n).

Lentiviral infection

The lentiviral vector containing the sequences of the shRNA of Cav3.1 (TRCN0000044239), Cav3.2 (TRCN0000044209), Snail1 (TRCN0000063818) and control (shRNA SCR; MFCD07785395) were from Sigma. The lentiviral vector comprising the sequence of shRNA of ATG5 was kindly provided by Yeramian A. We used pLX304-Snail1 (NM_005985.3) recombinant lentiviral plasmid to overexpress Snail1 in melanoma cells. See Supplemental Experimental Procedures for shRNA sequences and lentiviruses generation.

Wound healing

A confluent monolayer of cells was scratched with yellow tip. Thereafter, cells were treated and we captured an image of the scratch at time 0h and after 24h to calculate the percentage of the wound filled by cells. For time-lapse wound healing assay movies see Supplemental Experimental Procedures.

Single cell migration assay

Cells were plated at low density (6000 cell/cm²) to minimize cell-cell interactions. Cells were treated and capturing an image every 20 minutes for 20h. Cells were tracked using ImageJ

plugin and the accumulated distance (μm) and the velocity ($\mu\text{m}/\text{h}$) of the single cells were evaluated using Chemotaxis and Migration Tool (Ibidi).

Transwell experiments

We first treated the cells during 24h. Then, cells were trypsinized and plated in the upper chamber of the Transwell (8 μm pore, Falcon) coated with Matrigel in serum-free medium. We used 10% of FBS as a chemoattractant. After 24h, cells were fixed with paraformaldehyde 4% and stained with Hoechst (5 $\mu\text{g}/\text{ml}$). Finally, cells were pictured under an epifluorescence microscope (Leica), before and after the cotton swap and we counted (ImageJ) to have the percentage of the migrated cells.

Tissue Microarray and Immunohistochemical study

One tissue microarray (TMA) was constructed from 61 formalin-fixed, paraffin-embedded (FFPE) melanoma tumors (primary and metastatic Table S2). Assessment of TTCC immunostaining and LC3 were done as detailed in (Maiques et al., 2016). The antibodies used and IHC protocol of Snail1 and scoring see Supplemental Experimental Procedures.

In silico studies

SNAI1 expression was analyzed in 243 human melanoma samples (109 BRAFV600E, 134 BRAFWT) from The Cancer Genome Atlas (TCGA) database (<http://cancergenome.nih.gov/>). Only samples with greater than 70% tumor cell content were considered. Normalized mRNA expression data were downloaded from cBioPortal (Cerami et al., 2012; Gao et al., 2013) and analyzed using GraphPad Prism.

Ethics statement

Studies using human samples were approved by the Ethics Committee on Clinical Investigation of the Hospital Universitari Arnau de Vilanova (HUAV, Lleida, Spain), and all patients gave their informed consent.

Statistical analysis

Statistical analysis was carried out using GraphPad Prism software. All data were expressed as mean \pm SD from at least three independent experiments. Statistical significance was checked by application of Kolmogorov-Smirnov normality test followed by *t*-test or ANOVA and Bonferroni test (parametric Test), or Mann-Whitney test or Kruskal-Wallis test (non-parametric test). *P*-values are indicated by asterisks **p*<0.05; ***p*<0.01; ****p*<0.001.

This article is protected by copyright. All rights reserved.

CONFLICT OF INTEREST

The authors declare no conflict of interest

ACKNOWLEDGEMENTS

Supported by grants from ISCIII/FEDER “Una manera de hacer Europa” (FIS-PI1200260 and PI1500711 to RMM, PI1301980 to JH and CIBERONC-CB16/12/0023 to XMG), Fundació la Marató de TV3 (FMTV 201331-30 to SP, -31 to RMM, and -32 to AF), Generalitat de Catalunya (2014/SGR138 to XMG); and Cancer Research UK grants C33043/A12065 and C33043/A24478 (VSM, JLO). OM holds a predoctoral fellowship from IRBLleida/Diputació de Lleida and CB a predoctoral fellowship from University of Lleida. AM holds a postdoctoral fellowship from AECC Scientific Foundation. IRH is supported by Marie Skłodowska-Curie Action (H2020-MSCA-IF-2014-EF-ST). Tumour samples were obtained with the support of Xarxa de Bancs de Tumors de Catalunya sponsored by Pla Director d'Oncologia de Catalunya (XBTC) and IRBLleida Biobank (B.0000682) and PLATAFORMA BIOBANCOS (PT13/0010/0014).

REFERENCES

- Amaravadi, R. K. (2011). Cancer. Autophagy in tumor immunity. *Science (New York, N.Y.)*, 334(6062), 1501–2. <http://doi.org/10.1126/science.1216428>
- Armstrong, J. L., Corazzari, M., Martin, S., Pagliarini, V., Falasca, L., Hill, D. S., ... Lovat, P. E. (2011). Oncogenic B-RAF signaling in melanoma impairs the therapeutic advantage of autophagy inhibition. *Clinical Cancer Research*, 17(8), 2216–2226. <http://doi.org/10.1158/1078-0432.CCR-10-3003>
- Banzi, M., De Blasio, S., Lallas, A., Longo, C., Moscarella, E., Alfano, R., & Argenziano, G. (2016). Dabrafenib: a new opportunity for the treatment of BRAF V600-positive melanoma. *OncoTargets and Therapy*, 9, 2725–33. <http://doi.org/10.2147/OTT.S75104>
- Bertrand, M., Petit, V., Jain, A., Amsellem, R., Johansen, T., Larue, L., ... Beau, I. (2015). SQSTM1/p62 regulates the expression of junctional proteins through epithelial-mesenchymal transition factors. *Cell Cycle*, 14(3), 364–374. <http://doi.org/10.4161/15384101.2014.987619>

- Boya, P., González-Polo, R.-A., Casares, N., Perfettini, J.-L., Dessen, P., Larochette, N., ... Kroemer, G. (2005). Inhibition of macroautophagy triggers apoptosis. *Molecular and Cellular Biology*, 25(3), 1025–40. <http://doi.org/10.1128/MCB.25.3.1025-1040.2005>
- Cano, A., Pérez-Moreno, M. A., Rodrigo, I., Locascio, A., Blanco, M. J., del Barrio, M. G., ... Nieto, M. A. (2000). The transcription factor Snail controls epithelial–mesenchymal transitions by repressing E-cadherin expression. *Nature Cell Biology*, 2(2), 76–83. <http://doi.org/10.1038/35000025>
- Carlino, M. S., Haydu, L. E., Kakavand, H., Menzies, A. M., Hamilton, A. L., Yu, B., ... Long, G. V. (2014). Correlation of BRAF and NRAS mutation status with outcome, site of distant metastasis and response to chemotherapy in metastatic melanoma. *British Journal of Cancer*, 111(2), 292–9. <http://doi.org/10.1038/bjc.2014.287>
- Cerami, E., Gao, J., Dogrusoz, U., Gross, B. E., Sumer, S. O., Aksoy, B. A., ... Schultz, N. (2012). The cBio cancer genomics portal: an open platform for exploring multidimensional cancer genomics data. *Cancer Discovery*, 2(5), 401–4. <http://doi.org/10.1158/2159-8290.CD-12-0095>
- Chin, L., Garraway, L. A., & Fisher, D. E. (2006). Malignant melanoma: genetics and therapeutics in the genomic era. *Genes & Development*, 20(16), 2149–2182. <http://doi.org/10.1101/gad.1437206>
- Corazzari, M., Rapino, F., Ciccocanti, F., Giglio, P., Antonioli, M., Conti, B., ... Piacentini, M. (2015). Oncogenic BRAF induces chronic ER stress condition resulting in increased basal autophagy and apoptotic resistance of cutaneous melanoma. *Cell Death and Differentiation*, 22(6), 946–58. <http://doi.org/10.1038/cdd.2014.183>
- Das, A., Pushparaj, C., Bahí, N., Sorolla, A., Herreros, J., Pamplona, R., ... Cantí, C. (2012). Functional expression of voltage-gated calcium channels in human melanoma. *Pigment Cell & Melanoma Research*, 25(2), 200–12. <http://doi.org/10.1111/j.1755-148X.2012.00978.x>
- Das, A., Pushparaj, C., Herreros, J., Nager, M., Vilella, R., Portero, M., ... Cantí, C. (2013). T-type calcium channel blockers inhibit autophagy and promote apoptosis of malignant melanoma cells. *Pigment Cell and Melanoma Research*, 26(6), 874–885. <http://doi.org/10.1111/pcmr.12155>
- Davies, H., Bignell, G. R., Cox, C., Stephens, P., Edkins, S., Clegg, S., ... Futreal, P. A. (2002).

Mutations of the BRAF gene in human cancer. *Nature*, 417(6892), 949–954.

<http://doi.org/10.1038/nature00766>

Dhomen, N., Reis-Filho, J. S., da Rocha Dias, S., Hayward, R., Savage, K., Delmas, V., ... Marais, R. (2009). Oncogenic Braf Induces Melanocyte Senescence and Melanoma in Mice.

Cancer Cell, 15(4), 294–303. <http://doi.org/10.1016/j.ccr.2009.02.022>

Dziegielewska, B., Gray, L. S., & Dziegielewski, J. (2014). T-type calcium channels blockers as new tools in cancer therapies. *Pflügers Archiv : European Journal of Physiology*, 466(4), 801–10. <http://doi.org/10.1007/s00424-014-1444-z>

Ekwueme, D. U., Guy, G. P., Li, C., Rim, S. H., Parelkar, P., & Chen, S. C. (2011). The health burden and economic costs of cutaneous melanoma mortality by race/ethnicity-United States, 2000 to 2006. *Journal of the American Academy of Dermatology*, 65(5 Suppl 1), S133-43. <http://doi.org/10.1016/j.jaad.2011.04.036>

Gao, J., Aksoy, B. A., Dogrusoz, U., Dresdner, G., Gross, B., Sumer, S. O., ... Schultz, N. (2013). Integrative analysis of complex cancer genomics and clinical profiles using the cBioPortal. *Science Signaling*, 6(269), pl1. <http://doi.org/10.1126/scisignal.2004088>

Giglio, P., Fimia, G. M., Lovat, P. E., Piacentini, M., & Corazzari, M. (2015). Fateful music from a talented orchestra with a wicked conductor: Connection between oncogenic BRAF, ER stress, and autophagy in human melanoma. *Molecular & Cellular Oncology*, 2(3), e995016. <http://doi.org/10.4161/23723556.2014.995016>

Gray-Schopfer, V., Wellbrock, C., & Marais, R. (2007). Melanoma biology and new targeted therapy. *Nature*, 445(7130), 851–7. <http://doi.org/10.1038/nature05661>

Griewank, K. G., Scolyer, R. A., Thompson, J. F., Flaherty, K. T., Schadendorf, D., & Murali, R. (2014). Genetic alterations and personalized medicine in melanoma: progress and future prospects. *Journal of the National Cancer Institute*, 106(2), djt435. <http://doi.org/10.1093/jnci/djt435>

Hao, L., Ha, J. R., Kuzel, P., Garcia, E., & Persad, S. (2012). Cadherin switch from E- to N-cadherin in melanoma progression is regulated by the PI3K/PTEN pathway through Twist and Snail. *British Journal of Dermatology*, 166(6), 1184–1197. <http://doi.org/10.1111/j.1365-2133.2012.10824.x>

Hao, M., Song, F., Du, X., Wang, G., Yang, Y., Chen, K., & Yang, J. (2015). Advances in targeted

- therapy for unresectable melanoma: new drugs and combinations. *Cancer Letters*, 359(1), 1–8. <http://doi.org/10.1016/j.canlet.2014.12.050>
- Jakob, J. A., Bassett, R. L., Ng, C. S., Curry, J. L., Joseph, R. W., Alvarado, G. C., ... Davies, M. A. (2012). NRAS mutation status is an independent prognostic factor in metastatic melanoma. *Cancer*, 118(16), 4014–23. <http://doi.org/10.1002/cncr.26724>
- Kenific, C. M., Thorburn, A., & Debnath, J. (2010). Autophagy and metastasis: another double-edged sword. *Current Opinion in Cell Biology*, 22(2), 241–245. <http://doi.org/10.1016/j.ceb.2009.10.008>
- Kraya, A. A., Piao, S., Xu, X., Zhang, G., Herlyn, M., Gimotty, P., ... Speicher, D. W. (2015). Identification of secreted proteins that reflect autophagy dynamics within tumor cells. *Autophagy*, 11(1), 60–74. <http://doi.org/10.4161/15548627.2014.984273>
- Kroemer, G., Mariño, G., & Levine, B. (2010). Autophagy and the integrated stress response. *Molecular Cell*, 40(2), 280–93. <http://doi.org/10.1016/j.molcel.2010.09.023>
- Kudo-Saito, C., Shirako, H., Takeuchi, T., & Kawakami, Y. (2009). Cancer Metastasis Is Accelerated through Immunosuppression during Snail-Induced EMT of Cancer Cells. *Cancer Cell*, 15(3), 195–206. <http://doi.org/10.1016/j.ccr.2009.01.023>
- Lee, J. S., DuBois, S. G., Coccia, P. F., Bleyer, A., Olin, R. L., & Goldsby, R. E. (2016). Increased risk of second malignant neoplasms in adolescents and young adults with cancer. *Cancer*, 122(1), 116–23. <http://doi.org/10.1002/cncr.29685>
- Long, G. V., Menzies, A. M., Nagrial, A. M., Haydu, L. E., Hamilton, A. L., Mann, G. J., ... Kefford, R. F. (2011). Prognostic and Clinicopathologic Associations of Oncogenic BRAF in Metastatic Melanoma. *Journal of Clinical Oncology*, 29(10), 1239–1246. <http://doi.org/10.1200/JCO.2010.32.4327>
- Lu, H., Liu, S., Zhang, G., Kwong, L. N., Zhu, Y., Miller, J. P., ... Guo, W. (2016). Oncogenic BRAF-Mediated Melanoma Cell Invasion. *Cell Reports*, 15(9), 2012–24. <http://doi.org/10.1016/j.celrep.2016.04.073>
- Lv, C., Dai, H., Sun, M., Zhao, H., Wu, K., Zhu, J., ... Xue, C. (2017). Mesenchymal stem cells induce epithelial mesenchymal transition in melanoma by paracrine secretion of transforming growth factor- β . *Melanoma Research*, 27(2), 74–84. <http://doi.org/10.1097/CMR.0000000000000325>

- Ma, X.-H., Piao, S.-F., Dey, S., McAfee, Q., Karakousis, G., Villanueva, J., ... Amaravadi, R. K. (2014). Targeting ER stress-induced autophagy overcomes BRAF inhibitor resistance in melanoma. *The Journal of Clinical Investigation*, 124(3), 1406–17. <http://doi.org/10.1172/JCI70454>
- Ma, X.-H., Piao, S., Wang, D., McAfee, Q. W., Nathanson, K. L., Lum, J. J., ... Amaravadi, R. K. (2011). Measurements of tumor cell autophagy predict invasiveness, resistance to chemotherapy, and survival in melanoma. *Clinical Cancer Research : An Official Journal of the American Association for Cancer Research*, 17(10), 3478–89. <http://doi.org/10.1158/1078-0432.CCR-10-2372>
- Macià, A., Herreros, J., Martí, R. M., & Cantí, C. (2015). Calcium channel expression and applicability as targeted therapies in melanoma. *BioMed Research International*, 2015, 587135. <http://doi.org/10.1155/2015/587135>
- Maddodi, N., Huang, W., Havighurst, T., Kim, K., Longley, B. J., & Setaluri, V. (2010). Induction of autophagy and inhibition of melanoma growth in vitro and in vivo by hyperactivation of oncogenic BRAF. *J Invest Dermatol*, 130(6), 1657–1667. <http://doi.org/10.1038/jid.2010.26>
- Maes, H., & Agostinis, P. (2014). Autophagy and mitophagy interplay in melanoma progression. *Mitochondrion*, 19 Pt A, 58–68. <http://doi.org/10.1016/j.mito.2014.07.003>
- Maes, H., Kuchnio, A., Peric, A., Moens, S., Nys, K., DeBock, K., ... Carmeliet, P. (2014). Tumor vessel normalization by chloroquine independent of autophagy. *Cancer Cell*, 26(2), 190–206. <http://doi.org/10.1016/j.ccr.2014.06.025>
- Maiques, O., Macià, A., Moreno, S., Barceló, C., Santacana, M., Veà, A., ... Martí, R. M. (2016). Immunohistochemical analysis of T-type calcium channels in acquired melanocytic nevi and melanoma. *The British Journal of Dermatology*. <http://doi.org/10.1111/bjd.15121>
- Martin, S., Dudek-Perić, A. M., Maes, H., Garg, A. D., Gabrysiak, M., Demirsoy, S., ... Agostinis, P. (2015). Concurrent MEK and autophagy inhibition is required to restore cell death associated danger-signalling in Vemurafenib-resistant melanoma cells. *Biochemical Pharmacology*, 93(3), 290–304. <http://doi.org/10.1016/j.bcp.2014.12.003>
- Massoumi, R., Kuphal, S., Hellerbrand, C., Haas, B., Wild, P., Spruss, T., ... Bosserhoff, A. K. (2009). Down-regulation of CYLD expression by Snail promotes tumor progression in malignant melanoma. *The Journal of Experimental Medicine*, 206(1), 221–232.

<http://doi.org/10.1084/jem.20082044>

- Mizushima, N., & Komatsu, M. (2011). Autophagy: Renovation of Cells and Tissues. *Cell*, *147*(4), 728–741. <http://doi.org/10.1016/j.cell.2011.10.026>
- Mizushima, N., Yoshimori, T., & Levine, B. (2010). Methods in mammalian autophagy research. *Cell*, *140*(3), 313–26. <http://doi.org/10.1016/j.cell.2010.01.028>
- Mowers, E. E., Sharifi, M. N., & Macleod, K. F. (2016). Autophagy in cancer metastasis. *Oncogene*. <http://doi.org/10.1038/onc.2016.333>
- Muqbil, I., Wu, J., Aboukameel, A., Mohammad, R. M., & Azmi, A. S. (2014). Snail nuclear transport: the gateways regulating epithelial-to-mesenchymal transition? *Seminars in Cancer Biology*, *27*, 39–45. <http://doi.org/10.1016/j.semcancer.2014.06.003>
- Narita, M., Young, A. R. J., Arakawa, S., Samarajiwa, S. A., Nakashima, T., Yoshida, S., ... Narita, M. (2011). Spatial Coupling of mTOR and Autophagy Augments Secretory Phenotypes. *Science*, *332*(6032), 966–970. <http://doi.org/10.1126/science.1205407>
- Olmeda, D., Jordá, M., Peinado, H., Fabra, Á., & Cano, A. (2007). Snail silencing effectively suppresses tumour growth and invasiveness. *Oncogene*, *26*(13), 1862–1874. <http://doi.org/10.1038/sj.onc.1209997>
- Pearlman, R. L., Montes de Oca, M. K., Pal, H. C., & Afaq, F. (2017). Potential therapeutic targets of epithelial–mesenchymal transition in melanoma. *Cancer Letters*, *391*, 125–140. <http://doi.org/10.1016/j.canlet.2017.01.029>
- Pollack, L. A., Li, J., Berkowitz, Z., Weir, H. K., Wu, X.-C., Ajani, U. A., ... Pollack, B. P. (2011). Melanoma survival in the United States, 1992 to 2005. *Journal of the American Academy of Dermatology*, *65*(5 Suppl 1), S78-86. <http://doi.org/10.1016/j.jaad.2011.05.030>
- Poser, I., Domínguez, D., de Herreros, A. G., Varnai, A., Buettner, R., & Bosserhoff, A. K. (2001). Loss of E-cadherin Expression in Melanoma Cells Involves Up-regulation of the Transcriptional Repressor Snail. *Journal of Biological Chemistry*, *276*(27), 24661–24666. <http://doi.org/10.1074/jbc.M011224200>
- Pyo, J.-O., Jang, M.-H., Kwon, Y.-K., Lee, H.-J., Jun, J.-I., Woo, H.-N., ... Jung, Y.-K. (2005). Essential roles of Atg5 and FADD in autophagic cell death: dissection of autophagic cell death into vacuole formation and cell death. *The Journal of Biological Chemistry*, *280*(21), 20722–9. <http://doi.org/10.1074/jbc.M413934200>

- Ríos, L., Nagore, E., López, J. L., Redondo, P., Martí, R. M., Fernández-de-Misa, R., & Soler, B. (2013). Registro nacional de melanoma cutáneo. Características del tumor en el momento del diagnóstico: 15 años de experiencia. *Actas Dermo-Sifiliográficas*, *104*(9), 789–799. <http://doi.org/10.1016/j.ad.2013.02.003>
- Sahani, M. H., Itakura, E., & Mizushima, N. (2014). Expression of the autophagy substrate SQSTM1/p62 is restored during prolonged starvation depending on transcriptional upregulation and autophagy-derived amino acids. *Autophagy*, *10*(3), 431–41. <http://doi.org/10.4161/auto.27344>
- Salah, F. S., Ebbinghaus, M., Muley, V. Y., Zhou, Z., Al-Saadi, K. R. D., Pacyna-Gengelbach, M., ... Petersen, I. (2016). Tumor suppression in mice lacking GABARAP, an Atg8/LC3 family member implicated in autophagy, is associated with alterations in cytokine secretion and cell death. *Cell Death and Disease*, *7*(4), e2205. <http://doi.org/10.1038/cddis.2016.93>
- Sandri, S., Fai??o-Flores, F., Tiago, M., Pennacchi, P. C., Massaro, R. R., Alves-Fernandes, D. K., ... Maria-Engler, S. S. (2016). Vemurafenib resistance increases melanoma invasiveness and modulates the tumor microenvironment by MMP-2 upregulation. *Pharmacological Research*, *111*, 523–533. <http://doi.org/10.1016/j.phrs.2016.07.017>
- Sharifi, M. N. N., Mowers, E. E. E., Drake, L. E. E., Collier, C., Chen, H., Zamora, M., ... Macleod, K. F. F. (2016). Autophagy Promotes Focal Adhesion Disassembly and Cell Motility of Metastatic Tumor Cells through the Direct Interaction of Paxillin with LC3. *Cell Reports*, *15*(8), 1660–1672. <http://doi.org/10.1016/j.celrep.2016.04.065>
- Thiery, J. P. (2002). Epithelial–mesenchymal transitions in tumour progression. *Nature Reviews Cancer*, *2*(6), 442–454. <http://doi.org/10.1038/nrc822>
- Vu, H. L., & Aplin, A. E. (2016). Targeting mutant NRAS signaling pathways in melanoma. *Pharmacological Research*, *107*, 111–116. <http://doi.org/10.1016/j.phrs.2016.03.007>
- Xie, X., Koh, J. Y., Price, S., White, E., & Mehnert, J. M. (2015). Atg7 Overcomes Senescence and Promotes Growth of BrafV600E-Driven Melanoma. *Cancer Discov*, *5*(4), 410–423. <http://doi.org/10.1158/2159-8290.CD-14-1473>

LEGEND FOR FIGURES

Figure 1: TTCCs are expressed in melanoma cell lines and TTCC blockers inhibit macroautophagy. qRT-PCR of a) Cav3.1, b) Cav3.2 and c) Cav3.3 in BRAFV600E or NRAS mutated melanoma cell lines and normalized to GAPDH expression. The mRNA levels from melanocytes (HEMn-LP) are shown for comparison. Comparison of the mRNA levels of (d) Cav3.1, (e) Cav3.2 and (f) Cav3.3 between cell line groups. The statistical analysis used was Mann Whitney test, (*p<0.05; n.s non-significant). g) Analysis of LC3I/II by WB from total protein lysates. WB analysis to test p62 and LC3 protein levels from h) BRAFV600E and i) NRAS mutant melanoma cells exposed to Mibefradil (Mib, 10 μ M) and Pimozide (Pim, 10 μ M) for 24h. j) BRAFV600E and k) NRAS mutant melanoma cells treated with CQ (25 μ M) for 24h. β -actin was used as a loading control. l) Immunofluorescence images and graphs of LC3B positive *puncta* in M3 (BRAFV600E) and Skmel-147 (NRASQ61R) cell lines in untreated, Mib or CQ treatments. AP: Autophagosomes. Statistical analysis was performed using ANOVA and Bonferroni tests (*p<0.05; **p<0.01; ***p<0.001; n.s., non-significant).

Figure 2: Blocking macroautophagy inhibits migration of BRAFV600E melanoma cells. Representative pictures and graphs of wound healing assay of (a-b) BRAFV600E and (c-d) NRAS mutant cells treated with Mibefradil (10 μ M, Mib), Pimozide (10 μ M, Pim) and CQ (25 μ M) during 24h. Panels on the left of each cell line represent the percentage of wound closure as a result of at least three independent experiments. Panels on the right represent the healing speed (μ m²/h) of cells after treatment compared to the control analyzed by estimated linear regression. e) WB analysis shows the downregulation of ATG5 and LC3I/II levels. β -actin was used as a loading control. Percentage of wound closure in (f) M3 and (g) WM-1366 cells control (Vector) or upon ATG5 silencing (shATG5). Statistical analysis was performed using ANOVA and Bonferroni tests or *t*-test (*p<0.05; **p<0.01; ***p<0.001; n.s., non-significant).

Figure 3: Mibefradil and CQ reduce single cell migration in BRAFV600E melanoma cells. Cell tracking analysis was carried out for 24h at a rate of 1 frame per 20 minutes. The total accumulated length migrated (μ m) and the migration speed (μ m/h) of treated and untreated cells was analyzed in (a-b) BRAFV600E and (c-d) NRAS mutant cells. Around 25 significant tracks of control and treated cells were plotted in the trajectory graphs in the right side of the figure. Trajectories of each group of cells were standardized to all begin at the same starting point. The statistical analysis used was ANOVA and Bonferroni tests (*p<0.05; **p<0.01; ***p<0.001).

Figure 4: Autophagy blockade and silencing of Cav3.1 and Cav3.2 reduce cell invasion in BRAFV600E melanoma cell lines. a) Representative images of nuclear Hoechst staining after the cotton swap (microscopic field x10). b) Percentage (%) of cells that invaded the Matrigel after treatment with Mib and CQ compared to the control. c-d) M3 and WM-1366 cells were infected with control lentiviruses (Vector, control) or lentiviruses expressing a shRNA of ATG5. c) Representative nuclear Hoechst staining of cells that invaded the Matrigel and (d) graph representing the % of invasive cells. e) Representative images of nuclear Hoechst staining after the cotton swap in M3 cell line infected with shRNA of Cav3.1 and Cav3.2 compared to control (Vector, scrambled shRNA) and f) Percentage (%) of invaded cells. Pictures magnification 10x. The statistical analysis used was ANOVA and Bonferroni test (*p<0.05; **p<0.01; ***p<0.001; n.s., non-significant).

Figure 5: Differential expression of Cav3.1, Cav3.2 and LC3 in melanoma depending on BRAF mutational status. Differential immunoexpression (Histoscore, mean±SD) and representative images of the immunostaining for (a-b) Cav3.1 (mean HS BRAFV600E/K vs WT: 85 vs 37,5), (c-d) Cav3.2 (mean HS BRAFV600E/K vs WT:147.5 and 146.6) and (e-f) LC3 (mean HS BRAFV600E/K vs WT: 84 vs 44,6) analyzed in BRAF mutant melanoma biopsies compared to BRAFWT melanoma samples. Pictures magnification 20x. The statistical analysis used was Mann Whitney test (*p<0.05; **p<0.01; ***p<0.001; n.s., non-significant).

Figure 6: BRAFV600 melanomas express higher levels of Snail1, which decrease upon autophagy blockade. a) WB and b) mRNA Snail1 levels between BRAFV600E and NRAS mutated melanoma cell lines. WB analysis of Snail1 in BRAFV600E and NRAS mutant cells treated with (c) Mibefradil, Pimozide or (d) CQ. WB analysis of Snail1 in BRAFV600E cells silenced for (e) ATG5, (f) Cav3.1, Cav3.2 and (g) Snail1. (g) Wound healing assay and (h) Transwell assay of BRAFV600E after Snail1 silencing vs control cells (vector). i) WB analysis of LC3I/II and P62 in PLX-Snail1 vs PLX-vector cells. Endogenous immunofluorescence of LC3B when cells were treated with (j) Chloroquine (CQ, 3h) or Mibefradil (Mib, 24h). k) Wound healing assay, (l) Single Cell migration assay and (m) Transwell assay of PLX-Snail1 vs PLX-vector cells treated with (k,m,) Mibefradil 10µM or (l) 5µM and (k) CQ 25µM during 24h. Statistical analysis was performed using ANOVA and Bonferroni tests (*p<0.05; **p<0.01; ***p<0.001; n.s., non-significant). (n) SNAI1 expression in BRAFV600E and BRAFWT melanoma samples using normalized mRNA expression data from TCGA database. o) Graph and representative images (magnifications 10x and 40x) of nuclear 4-tiered (0-3) score immunostaining of Snail1 in biopsies with BRAF characterized mutation. The statistical analysis used was Mann Whitney test (*p<0.05; **p<0.01; ***p<0.001; n.s., non-significant).

FIGURE 1

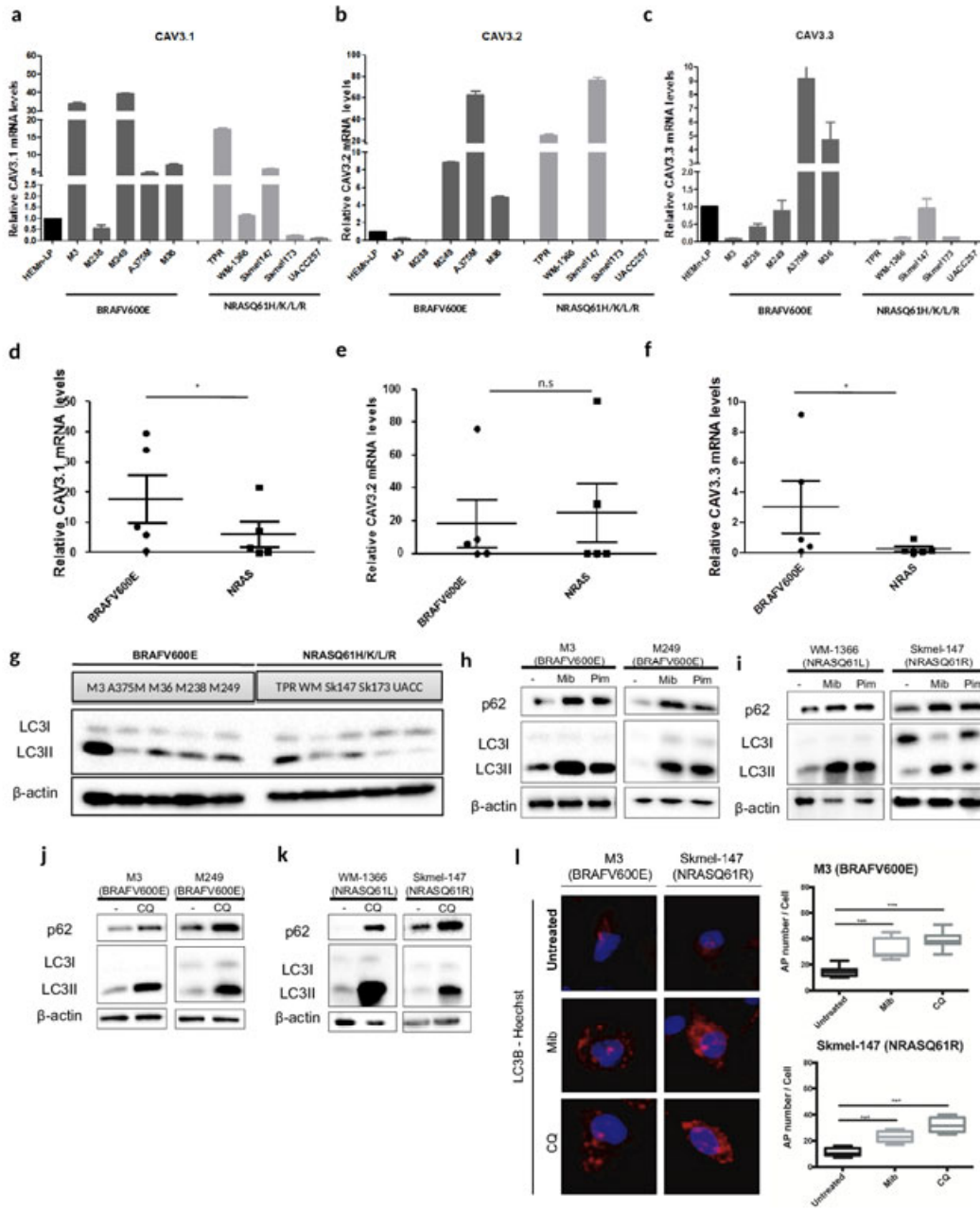


FIGURE 2

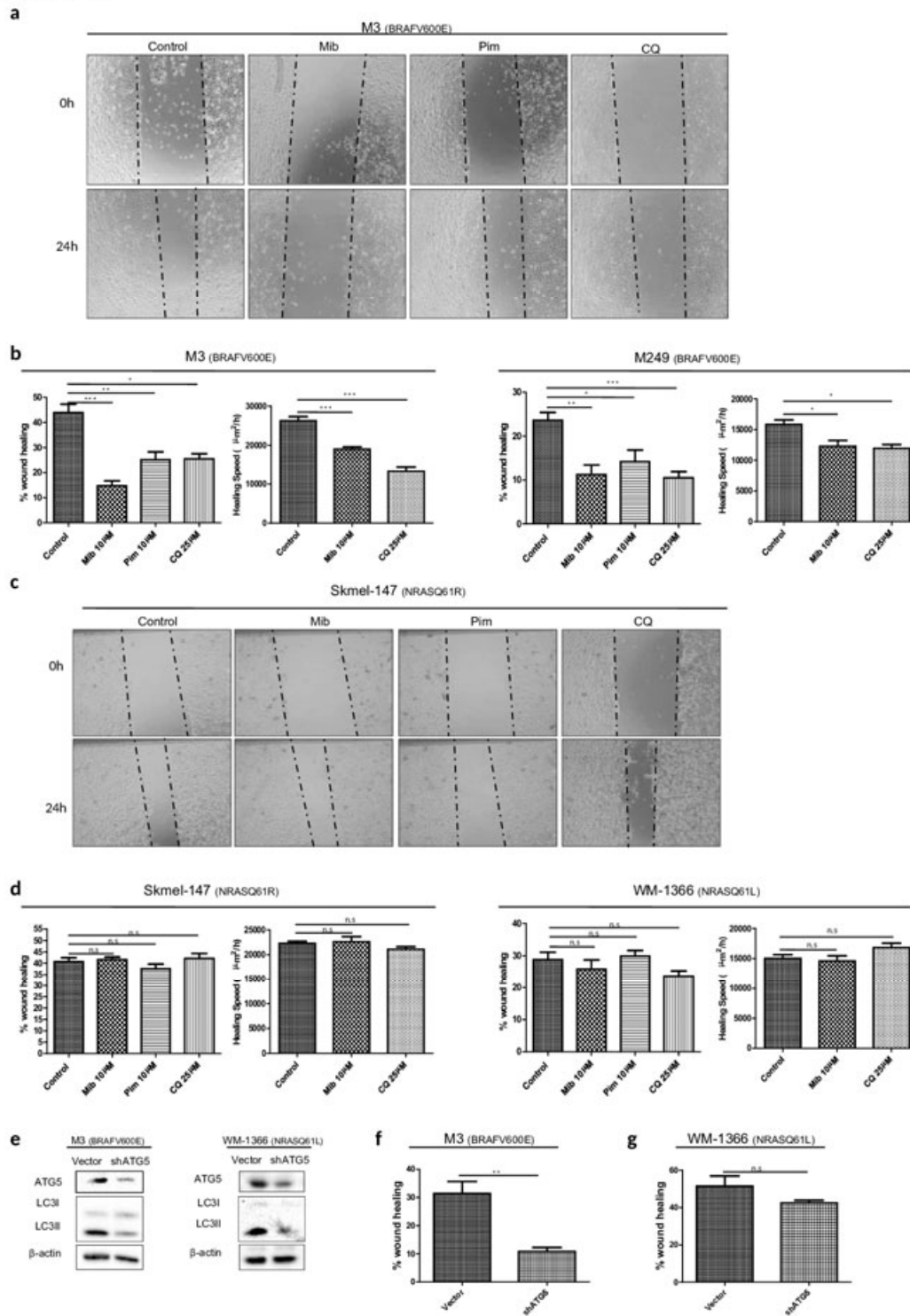


FIGURE 3

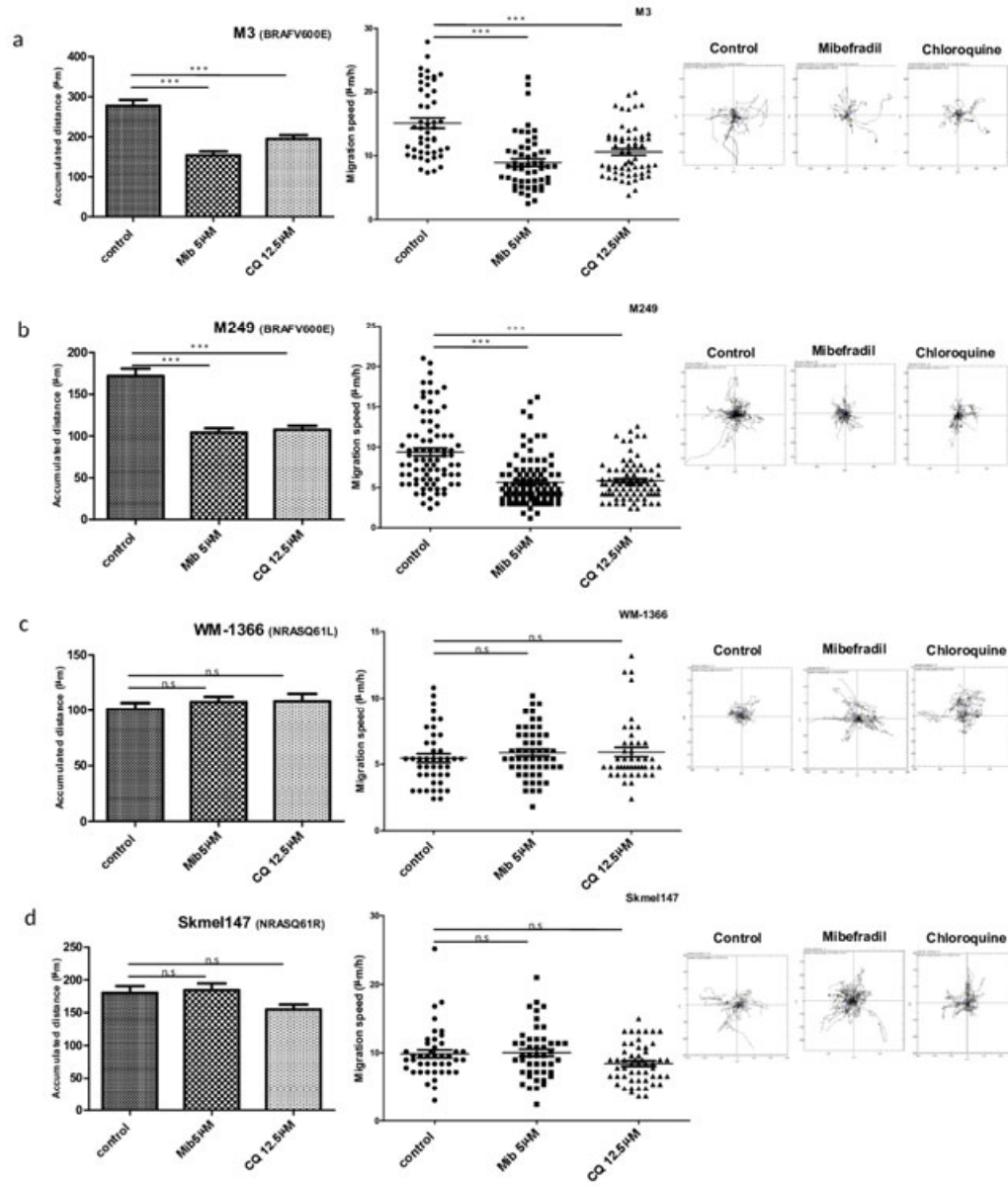


FIGURE 4

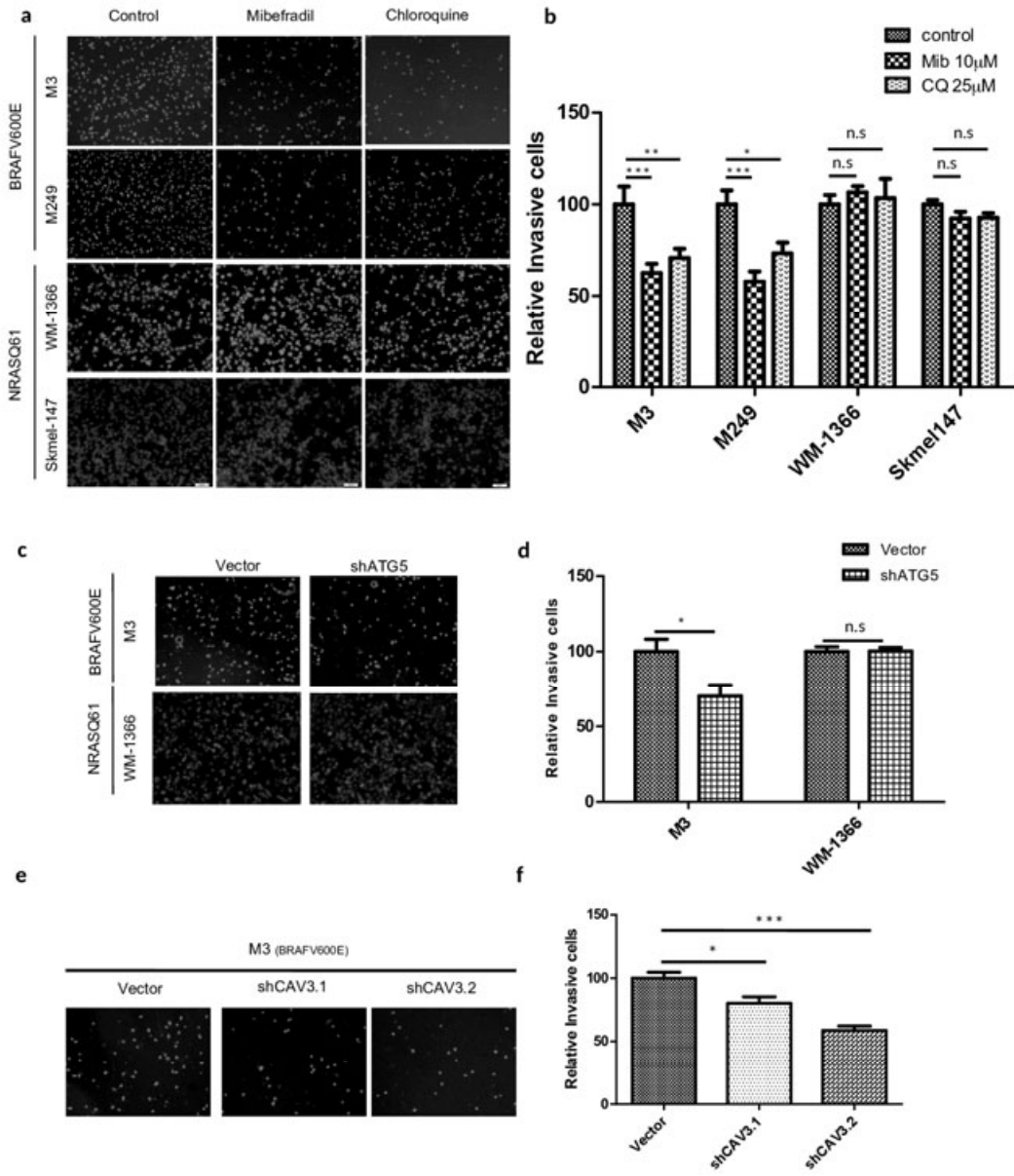


FIGURE 5

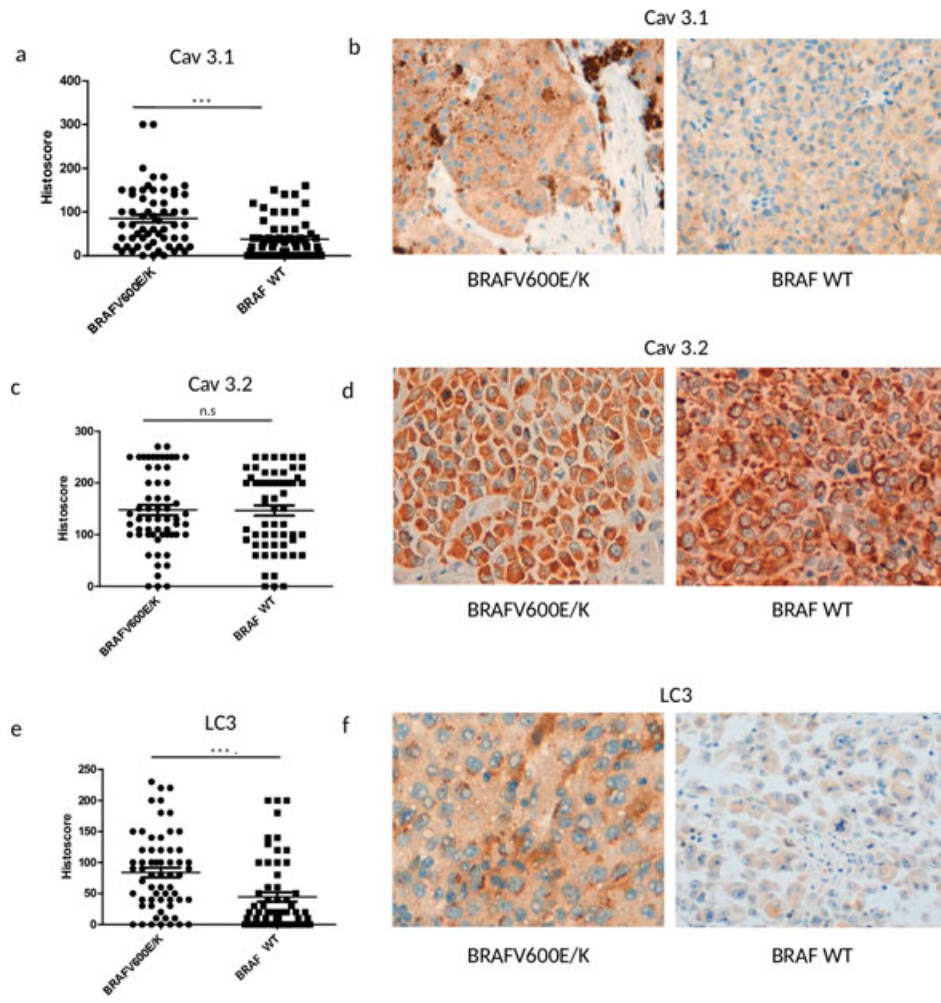


FIGURE 6

